Supplemental Materials

Molecular Biology of the Cell

Stewart-Ornstein et al.

SUPPLEMENTAL NOTE 1

This note provides an overview of our computational methods.

Negative feedback model The main interactions in the PKA regulatory pathways are depicted in Figure 3A. We model these interactions by

$$\frac{\mathrm{d}}{\mathrm{d}t}\,\mathrm{PKAa} = p_9\,\mathrm{cAMP}(\mathrm{PKAt}-\mathrm{PKAa}) - p_{10}\,\mathrm{PKAa} \tag{0.1a}$$

$$\frac{\mathrm{d}}{\mathrm{d}t}\,\mathrm{cAMP} = p_{23}u(t) + p_{11}\,\mathrm{RASa} + p_{10}\,\mathrm{PKAa} - \frac{p_{12}\,\mathrm{cAMP}}{\mathrm{cAMP}+p_{13}} - \frac{p_{14}\,\mathrm{cAMP}}{\mathrm{cAMP}+p_{15}p_{13}} - p_9\,\mathrm{cAMP}(\mathrm{PKAt}-\mathrm{PKAa}) \tag{0.1b}$$

$$\frac{\mathrm{d}}{\mathrm{d}t}\,\mathrm{RASa} = p_{16}\frac{(\mathrm{RASt}-\mathrm{RASa})\,\mathrm{CDC25}}{\mathrm{RASt}-\mathrm{RASa}+p_{17}} - p_{18}\frac{\mathrm{RASa}}{\mathrm{RASa}+p_{19}} \tag{0.1c}$$

$$\frac{\mathrm{d}}{\mathrm{d}t}\,\mathrm{CDC25} = p_{22} - p_{20}\frac{\mathrm{PKAa}\,\mathrm{CDC25}}{\mathrm{CDC25}+p_{21}} \tag{0.1d}$$

$$\frac{\mathrm{d}}{\mathrm{d}t}\,\mathrm{MSNn} = p_2\frac{\mathrm{MSNt}-\mathrm{MSNn}}{\mathrm{MSNt}-\mathrm{MSNn}+p_3} - p_4\frac{\mathrm{PKAa}\,\mathrm{MSNn}}{\mathrm{MSNn}+p_5} \tag{0.1e}$$

$$\mathrm{output} = p_1\frac{\mathrm{MSNn}+p_0}{\mathrm{MSNt}-\mathrm{MSNn}+p_0}. \tag{0.1f}$$

In these equations, PKAa and RASa represent protein activities, cAMP and CDC25 represent the concentration of the small molecule and protein respectively, MSNn is the concentration of nuclear Msn2, and $u(t)$ represents blue light intensity. The model is characterized by 24 parameters, including the 21 shown above as well as three parameters representing total protein concentrations: $p_6 = \mathrm{MSNt}, p_7 = \mathrm{RASt}, p_8 = \mathrm{PKAt}$.

Most of activation/inactivation and production/degradation terms are modeled by Michaelis-Menten kinetics, including the kinetics of Msn2 shuttling in/out of the nucleus. The interaction of PKA with cAMP, however, is modeled as a binding reaction. Inactive PKA is known to be a heterotetramer composed of a dimer of catalytic subunits and a dimer of regulatory subunits. cAMP is thought to activate the catalytic subunits by binding to and releasing the regulatory subunits. Here we assume that 2 cAMP molecules bind simultaneously and non-cooperatively to 2 regulatory subunits to release 2 catalytic subunits. Hence there is a 1:1 relationship between active catalytic subunits and cAMP molecules. Further, cAMP production is explicitly modeled as having two components dependent on Ras and blue light u.

Finally the output represents nuclear localization of Msn2, defined as the ratio of nuclear Msn2 to cytoplasmic Msn2, and is modeled as a rational function of Msn2n as in equation (0.1f). Here p_1 allows the output to be scaled version of Msn2 while p_0 accounts for background intensity.

The equations were numerically solved by the LSODE solver for stiff differential equations via the python package odespy [1].

Open loop model The open loop model replaces equation (0.1d) with

$$\frac{\mathrm{d}}{\mathrm{d}t}\,\mathrm{CDC25} = p_{22} - p_{20}\frac{\mathrm{CDC25}}{\mathrm{CDC25}+p_{21}} \tag{0.1d*}$$

Fitting Fits of experimental data to the feedback model (Figures 2 and 3; Supplemental Figure 7) and the open loop model (Figure 2; Supplemental Figure 3) were obtained by the three step procedure:

1. Sample parameters log uniformly with the requirements:

   - Rates/concentrations are sampled between 10^{-4} and 10^4.
   - p_6 through p_8 are sampled between 10^0 and 10^4.
   - The input and output parameters: p_1 is sampled between 10^{-3} to 10^1; p_1 and p_{23} are sampled between 10^0 to 10^2.
   - $10^{.5} < p_{15} < 10^4$. This is to ensure that the Pde1 and Pde2 terms can be distinguished and have the correct relative affinities.

   For both models, $>10^7$ sets were sampled.

2. Use the result of step 1 as seed values for Nelder-Mead optimization to fit to the experimental wild type data. The objective function is the mean square error weighted by the standard deviations at each time point.

3. Use the result of step 2 as seed values for Nelder-Mead optimization to fit to all 4 experimental strains. The mutants are modeled by

   - ΔIra2: $p_{18} \leftarrow p_{18}/4$
   - ΔPde2: $p_{12} \leftarrow 0$
   - ΔPde1: $p_{14} \leftarrow 0$

   The objective function is the mean square error weighted by standard deviations, averaged over the 4 data sets, plus a penalty to encourage desired behavior. The penalty is a heuristic that takes a weighted average of three terms,

   - a term dependent on cAMP, to prevent the minimum cAMP concentration from reaching zero,
   - a term dependent on $\frac{\mathrm{dcAMP}}{\mathrm{d}t}|_{t=3^-}$, to encourage the system to equilibrate by 3 minutes, and
   - a function of the average standard deviation of all species concentration between 30 and 35 minutes, to penalize models that do not reach steady state 30 min after bPAC induction.

   The equations were numerically solved by the LSODE solver for stiff differential equations via the python package odespy [1]. Any fits outside the parameter ranges established in step 1 were discarded.

From this procedure, we found approximately 300 parameter sets for the feedback model that fit all the experimental data.

Frequency sweep The response of the wildtype system to an input with varying period was simulated with the 300 best parameters sets obtained from our three-step fitting procedure described above. The input to the system was identical to that used in experiments, as shown in Figure 4. The transfer function was found by identifying the peak Msn2 nuclear localization (measured with respect to steady state Msn2 nuclear

localization) and then plotting the peaks as a function of frequency. This computationally derived transfer function was then fit to the standard transfer function for first and second order linear systems,

$$H_1(f) = \frac{C}{\sqrt{1 + (f/f_{c1})^2}} \tag{0.2a}$$

$$H_2(f) = \frac{C}{\sqrt{(1 - (f/f_{c2})^2)^2 + (f/f_{c2}Q)^2}}, \tag{0.2b}$$

where f is frequency and C, f_c, and Q are fitted parameters. The second order transfer function provided a better fit and produced the values for median cutoff frequency with IQR reported in the main text. Fitting was performed by the curvefit function of the scipy package [2].

The simulated phase response was determined by computing the lag of the output peak with respect to the input peak, as a proportion of the input period. This was then scaled appropriately and plotted against the input frequency.

References

[1] Langtangen HP and Wang L. Odespy software package (2014).

[2] Jones E, Oliphant E, Peterson P, et al. SciPy: Open Source Scientific Tools for Python, 2001-

SUPPLEMENTAL TEXT

SUPPLEMENTAL DATASETS

Supplemental Datasets 1 and 2 are csv files containing the log base 10 of the parameter sets found by sampling parameters for the feedback and open loop models respectively and fitting the results to WT experimental data (nuclear localization measured in response to 3 minutes bPAC induction). Supplemental Dataset 3 is a csv file with those parameter sets that fit both WT and mutant data. Details of the fitting procedure are described in Supplemental Note 1.

SUPPLEMENTAL FIGURE LEGENDS

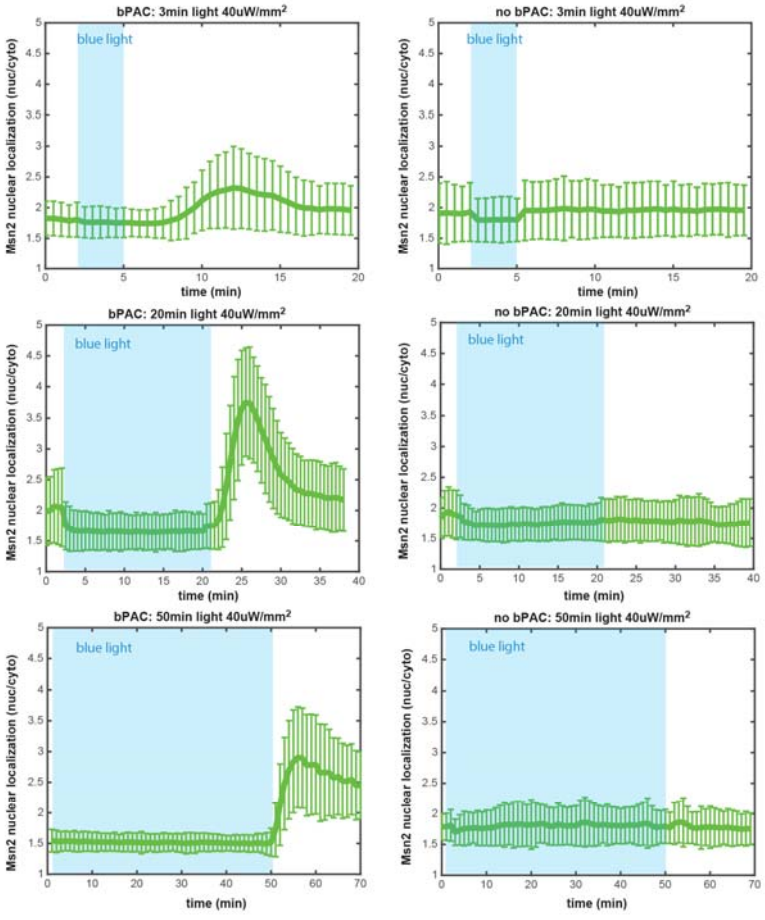

Supp Fig 1

Supp Figure 1: Extended blue light and fluorescent imaging exposure do not induce nuclear localization of Msn2. Time traces of Msn2-mCherry nuclear localization are plotted in green for cells with bPAC (left 3 panels) and cells

without bPAC (right 3 panels). The light blue shading indicates the time over which light is applied in the experiment. Blue light exposure span three different durations-- 3 minutes, 20 minutes, and 50 minutes-- at 40uW/mm^2 constant amplitude.

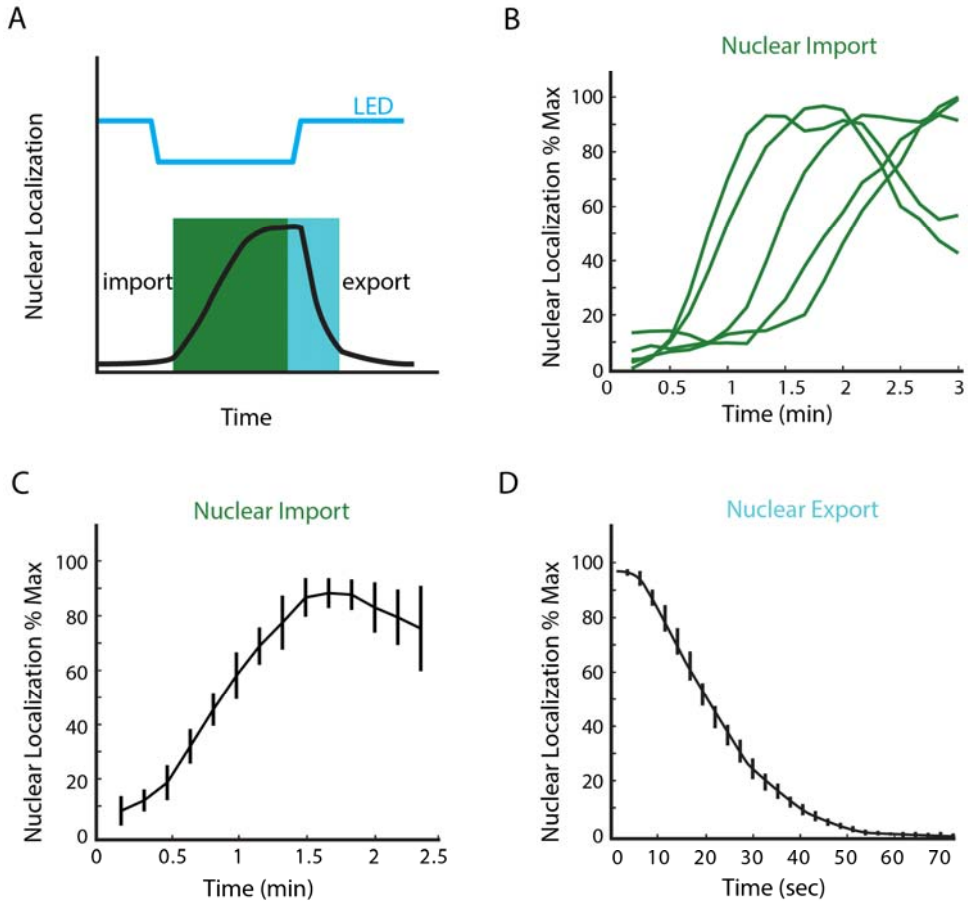

Supp Fig 2

Supp Figure 2: Real-time control of PKA activity with bPAC allows for quantification of Msn2 nuclear import and export rates. **(A)** Experimental blue light illumination protocol and expected Msn2 translocation pulse. The green shading represents the range considered as Msn2 nuclear import (B&C) and the light blue shading represents the range considered as Msn2 nuclear export (D). **(B & C)** Single cell traces of Msn2-mCherry nuclear import following shutoff of light pulse. When computationally synchronized as in (C), these traces can be used to estimate an average nuclear import rate of $T_{1/2}$~=30s. Error bars represent the standard deviation of three independent experiments. **(D)** Nuclear localization of Msn2-mCherry following reactivation of blue light. Nuclear export is estimated to have $T_{1/2}$ of ~20s. Nuclear export was more synchronous than nuclear import, and traces can therefore be immediately used for these export rate calculations.

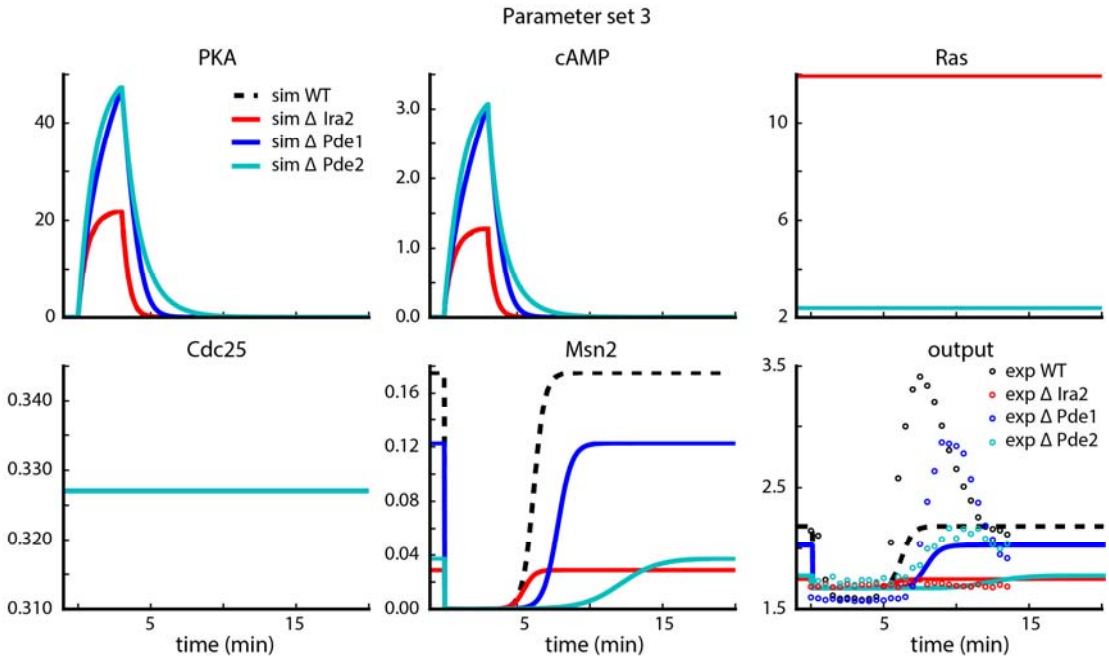

Supp Fig 3

Supp Figure 3: An open loop model does not recapitulate the transient pulse of Msn2 nuclear localization in response to a 3 minute transient blue light input starting at time t = 2 minutes. The open loop model was constructed by removing the Cdc25-PKA interaction and fitting to WT data. State variables (arbitrary units) for a representative fit are shown (solid lines). The different

solid line represent different strain background. Experimental data of Msn2 nuclear localization (output) is shown in circles. Other fitted parameter sets are available in Supplemental Dataset 2.

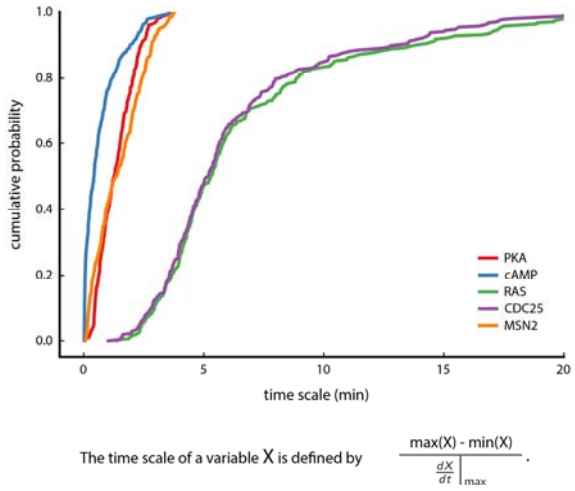

Supp Fig 4

Supp Figure 4: The negative feedback model exhibits a separation of time scales, with PKA, cAMP, and nuclear Msn2 responding faster on average than Cdc25 and Ras. Cumulative distribution functions for the time scale of each variable in the model for each of the parameter sets of Supplemental Dataset 3 obtained by fitting to WT and mutant Msn2 nuclear localization. For each fitted parameter set, each protein's time scale was computed by the formula shown (Segel, 1984).

A

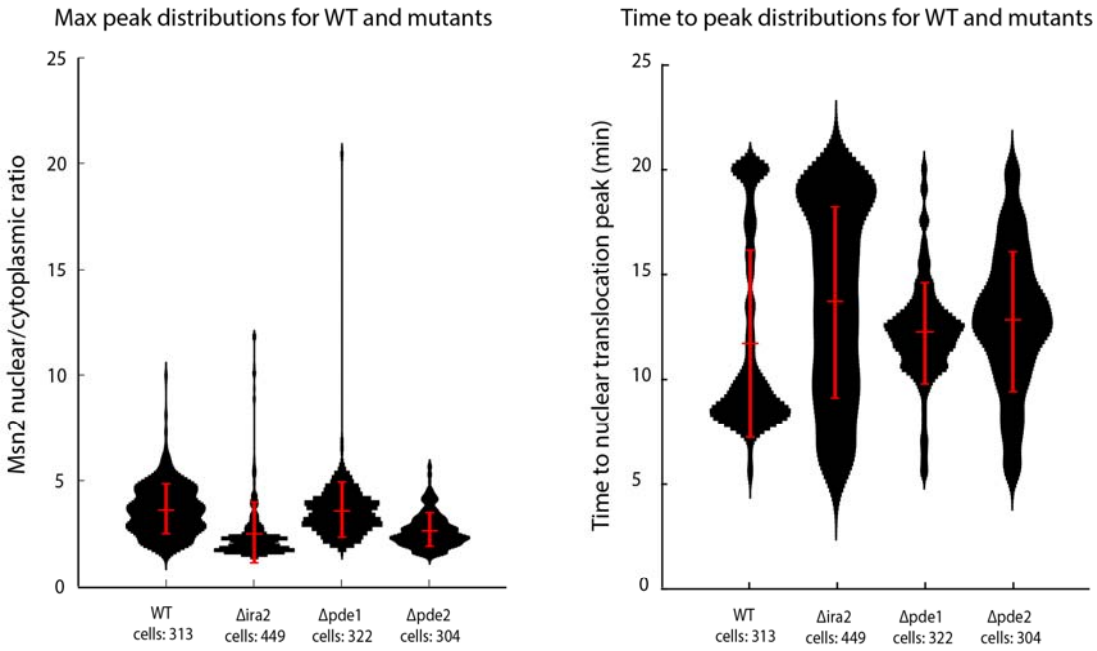

B

	WT	Δira2	Δpde1	Δpde2
Max peak (nuclear localization)	3.55	2.16*	3.43	2.44*
Time to peak (min)	10.5*	14*	12*	12.75*

* Two sample Kolmogorov-Smirnov test, p-value < 0.05

Supp Fig 5

Supp Figure 5: Distributions of time trace features (maximum peak and the time to peak of Msn2 nuclear localization) show that WT and mutant populations are distinct. **(A)** Single cell distributions of the time trace features, maximum peak and time to peak, are plotted for WT, *Δira1, Δira2, Δpde1* and *Δpde2* samples with median and the interquartile range shown (red). **(B)** The medians of single cell distributions for the max peak heights and time to peak are shown. The variability in the single cell data is attributed to a combination of natural biological variability to input signal and also technical noise. The two-sample Kolmogorov-Smirnov test was used to determine the significance of the difference in distributions of the WT and the deletions mutants. Asterisk signifies statistically significant (p<0.05) differences as compared to WT.

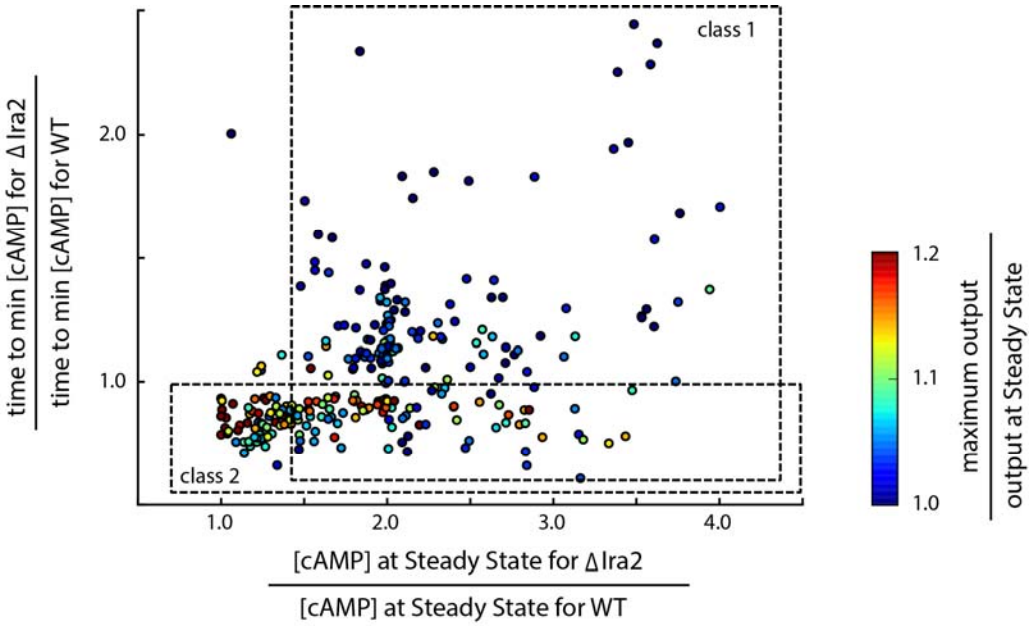

Supp Fig 6

Supp Figure 6: Fitted parameter sets from Supplemental Dataset 3 exhibit two non-exclusive features that explain the observed *Δira2* phenotype. Class 1 is

characterized by an increase in cAMP concentration at steady state and during bPAC application whereas class 2 is characterized by a fast attainment of the cAMP minimum. Both classes show a reduced Msn2 pulse for *Δira2*.

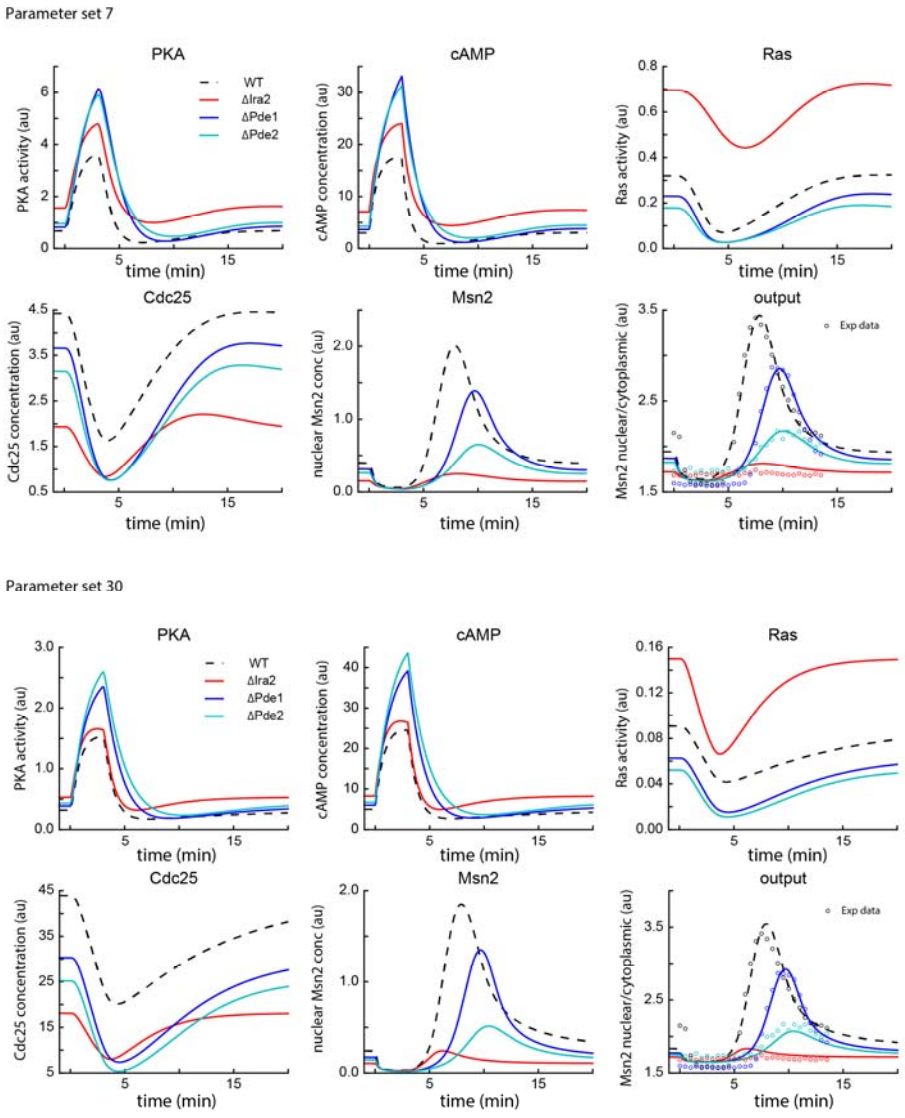

Supp Fig 7

Supp Figure 7: Simulated concentrations (arbitrary units) over time from the negative feedback model in response to a transient 3 minute pulse of blue light starting at time t = 2 minutes. Two parameter sets from Supplemental Dataset 3, obtained by fitting the negative feedback model to WT and mutant Msn2 nuclear localization measured during and after blue light illumination. The two chosen parameter sets are the same as those that generated the data for model plots of Figures 3 and 4.

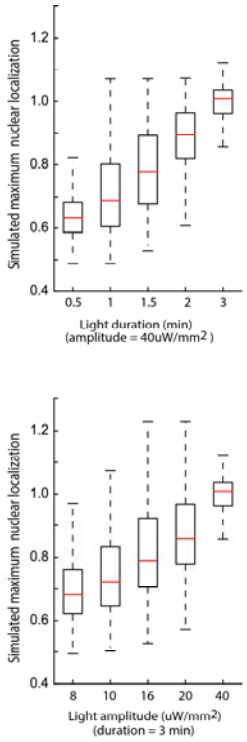

Supp Fig 8

Supp Figure 8: Msn2 peak nuclear localization simulated for the parameter sets of Supplemental Dataset 3 increases with light duration (top) and light amplitude (bottom). Data normalized so that the median of peak Msn2 in response to a blue light pulse of 3 minutes and 40uW/mm^2 is 1. The distributions are across the different parameter sets of Supplemental Dataset 3; boxes indicate quartiles with median in red.

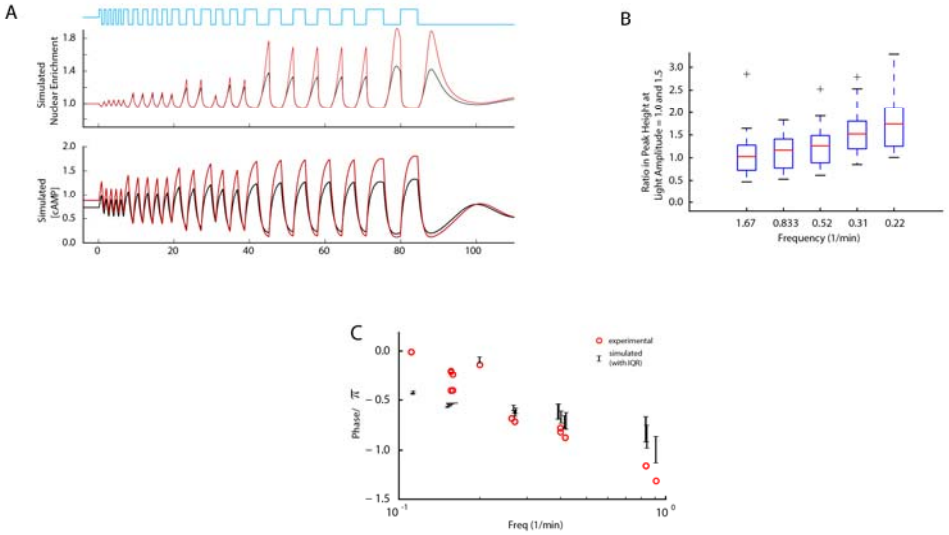

Supp Fig 9

Supp Figure 9(A) Simulated Msn2 nuclear enrichment and cAMP concentration in response to a light input with varying frequencies, when light amplitude is increased by a factor of 1.5 (red) relative to baseline (black). If bPAC input saturates, then the model underestimates cAMP production at high frequencies. The effect of this underestimation can be assessed by increasing the light input and observing the change at high frequencies. **(B)** The distribution of the change in peak height, as a function of input frequency, when the light input amplitude increases by a factor of 1.5. For the three highest frequencies, where the underestimation of cAMP production is most likely, the median change is close to one. **(C)** Phase response for simulated and experimental data shows general agreement.

SUPPLEMENTAL REFERENCES

Segel, L. *Modeling Dynamic Phenomena in Molecular and Cellular Biology*. Cambridge University Press (1984).